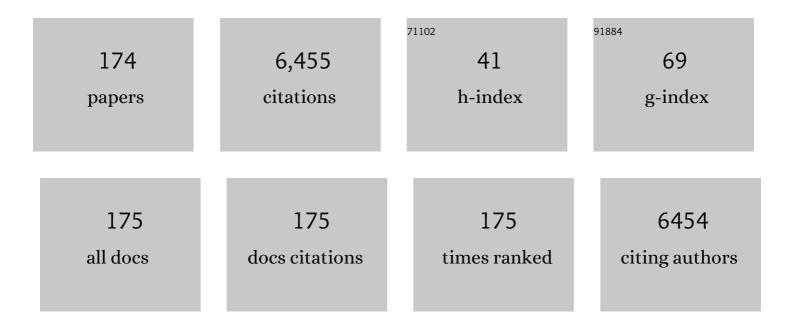
## **Ouyang Wei**

List of Publications by Year in descending order

Source: https://exaly.com/author-pdf/5196388/publications.pdf Version: 2024-02-01



#	Article	IF	CITATIONS
1	Increased plastic pollution due to COVID-19 pandemic: Challenges and recommendations. Chemical Engineering Journal, 2021, 405, 126683.	12.7	552
2	Persulfate-based advanced oxidation processes (AOPs) for organic-contaminated soil remediation: A review. Chemical Engineering Journal, 2019, 372, 836-851.	12.7	435
3	Heavy metal loss from agricultural watershed to aquatic system: A scientometrics review. Science of the Total Environment, 2018, 637-638, 208-220.	8.0	178
4	Properties comparison of biochars from corn straw with different pretreatment and sorption behaviour of atrazine. Bioresource Technology, 2013, 147, 338-344.	9.6	156
5	Combined impacts of land use and soil property changes on soil erosion in a mollisol area under long-term agricultural development. Science of the Total Environment, 2018, 613-614, 798-809.	8.0	138
6	Identification of sources of heavy metals in agricultural soils using multivariate analysis and GIS. Journal of Soils and Sediments, 2013, 13, 720-729.	3.0	129
7	Soil erosion dynamics response to landscape pattern. Science of the Total Environment, 2010, 408, 1358-1366.	8.0	124
8	The washing effect of precipitation on particulate matter and the pollution dynamics of rainwater in downtown Beijing. Science of the Total Environment, 2015, 505, 306-314.	8.0	124
9	Long-term vegetation landscape pattern with non-point source nutrient pollution in upper stream of Yellow River basin. Journal of Hydrology, 2010, 389, 373-380.	5.4	120
10	Soil erosion and sediment yield and their relationships with vegetation cover in upper stream of the Yellow River. Science of the Total Environment, 2010, 409, 396-403.	8.0	117
11	Spatial and seasonal variations of antibiotics in river waters in the Haihe River Catchment in China and ecotoxicological risk assessment. Environment International, 2019, 130, 104919.	10.0	104
12	Catalytic oxidation of contaminants by FeO activated peroxymonosulfate process: Fe(IV) involvement, degradation intermediates and toxicity evaluation. Chemical Engineering Journal, 2020, 382, 123013.	12.7	103
13	Vegetation NDVI Linked to Temperature and Precipitation in the Upper Catchments of Yellow River. Environmental Modeling and Assessment, 2012, 17, 389-398.	2.2	88
14	Occurrence, spatiotemporal variation, and ecological risk of antibiotics in the water of the semi-enclosed urbanized Jiaozhou Bay in eastern China. Water Research, 2020, 184, 116187.	11.3	83
15	Cascade Dam-Induced Hydrological Disturbance and Environmental Impact in the Upper Stream of the Yellow River. Water Resources Management, 2011, 25, 913-927.	3.9	78
16	Effects of Land Use Changes on the Ecosystem Service Values of a Reclamation Farm in Northeast China. Environmental Management, 2012, 50, 888-899.	2.7	77
17	Non-point source pollution dynamics under long-term agricultural development and relationship with landscape dynamics. Ecological Indicators, 2014, 45, 579-589.	6.3	74
18	Comparison of bio-augmentation and composting for remediation of oily sludge: A field-scale study in China. Process Biochemistry, 2005, 40, 3763-3768.	3.7	68

#	Article	IF	CITATIONS
19	Molecular Structure of Corncobâ€Đerived Biochars and the Mechanism of Atrazine Sorption. Agronomy Journal, 2013, 105, 773-782.	1.8	67
20	Assessment of soil erosion characteristics in response to temperature and precipitation in a freeze-thaw watershed. Geoderma, 2018, 328, 56-65.	5.1	63
21	An integrated package for drought monitoring, prediction and analysis to aid drought modeling and assessment. Environmental Modelling and Software, 2017, 91, 199-209.	4.5	62
22	Evaluating spatial interaction of soil property with nonâ€point source pollution at watershed scale: The phosphorus indicator in Northeast China. Science of the Total Environment, 2012, 432, 412-421.	8.0	60
23	Efficient removal of acetochlor pesticide from water using magnetic activated carbon: Adsorption performance, mechanism, and regeneration exploration. Science of the Total Environment, 2021, 778, 146353.	8.0	57
24	Effect of long-term agricultural cultivation and land use conversion on soil nutrient contents in the Sanjiang Plain. Catena, 2013, 104, 243-250.	5.0	56
25	A theoretical drought classification method for the multivariate drought index based on distribution properties of standardized drought indices. Advances in Water Resources, 2016, 92, 240-247.	3.8	56
26	Using river sediments to analyze the driving force difference for non-point source pollution dynamics between two scales of watersheds. Water Research, 2018, 139, 311-320.	11.3	56
27	Typical agricultural diffuse herbicide sorption with agricultural waste-derived biochars amended soil of high organic matter content. Water Research, 2016, 92, 156-163.	11.3	54
28	Activation of peroxymonosulfate by magnetic catalysts derived from drinking water treatment residuals for the degradation of atrazine. Journal of Hazardous Materials, 2019, 366, 402-412.	12.4	54
29	Synergistic impacts of land-use change and soil property variation on non-point source nitrogen pollution in a freeze–thaw area. Journal of Hydrology, 2013, 495, 126-134.	5.4	53
30	A review of diffuse pollution modeling and associated implications for watershed management in China. Journal of Soils and Sediments, 2017, 17, 1527-1536.	3.0	53
31	Distribution, sources, and ecological risks of potentially toxic elements in the Laizhou Bay, Bohai Sea: Under the long-term impact of the Yellow River input. Journal of Hazardous Materials, 2021, 413, 125429.	12.4	52
32	Temporal-spatial patterns of three types of pesticide loadings in a middle-high latitude agricultural watershed. Water Research, 2017, 122, 377-386.	11.3	51
33	Snowmelt water drives higher soil erosion than rainfall water in a mid-high latitude upland watershed. Journal of Hydrology, 2018, 556, 438-448.	5.4	51
34	Nonpoint Source Pollution Responses Simulation for Conversion Cropland to Forest in Mountains by SWAT in China. Environmental Management, 2008, 41, 79-89.	2.7	48
35	The influence of land-use change on the forms of phosphorus in soil profiles from the Sanjiang Plain of China. Geoderma, 2012, 189-190, 207-214.	5.1	48
36	Changing runoff due to temperature and precipitation variations in the dammed Jinsha River. Journal of Hydrology, 2020, 582, 124500.	5.4	48

#	Article	IF	CITATIONS
37	Occurrence, spatiotemporal distribution, and ecological risks of organophosphate esters in the water of the Yellow River to the Laizhou Bay, Bohai Sea. Science of the Total Environment, 2021, 787, 147528.	8.0	48
38	Temporal–spatial loss of diffuse pesticide and potential risks for water quality in China. Science of the Total Environment, 2016, 541, 551-558.	8.0	45
39	Temporal-spatial dynamics of vegetation variation on non-point source nutrient pollution. Ecological Modelling, 2009, 220, 2702-2713.	2.5	44
40	Occurrence, transportation, and distribution difference of typical herbicides from estuary to bay. Environment International, 2019, 130, 104858.	10.0	44
41	Seasonal relevance of agricultural diffuse pollutant with microplastic in the bay. Journal of Hazardous Materials, 2020, 396, 122602.	12.4	44
42	The effect on soil nutrients resulting from land use transformations in a freeze-thaw agricultural ecosystem. Soil and Tillage Research, 2013, 132, 30-38.	5.6	43
43	Quantitative risk assessment of the effects of drought on extreme temperature in eastern China. Journal of Geophysical Research D: Atmospheres, 2017, 122, 9050-9059.	3.3	43
44	Watershed soil Cd loss after long-term agricultural practice and biochar amendment under four rainfall levels. Water Research, 2017, 122, 692-700.	11.3	43
45	Sources, trophodynamics, contamination and risk assessment of toxic metals in a coastal ecosystem by using a receptor model and Monte Carlo simulation. Journal of Hazardous Materials, 2022, 424, 127482.	12.4	43
46	The non-point source pollution in livestock-breeding areas of the Heihe River basin in Yellow River. Stochastic Environmental Research and Risk Assessment, 2007, 21, 213-221.	4.0	40
47	Vegetation response to 30years hydropower cascade exploitation in upper stream of Yellow River. Communications in Nonlinear Science and Numerical Simulation, 2010, 15, 1928-1941.	3.3	40
48	Characteristics and secondary formation of water-soluble organic acids in PM1, PM2.5 and PM10 in Beijing during haze episodes. Science of the Total Environment, 2019, 669, 175-184.	8.0	40
49	Modeling urban storm rainfall runoff from diverse underlying surfaces and application for control design in Beijing. Journal of Environmental Management, 2012, 113, 467-473.	7.8	39
50	Occurrence, migration, and allocation of arsenic in multiple media of a typical semi-enclosed bay. Journal of Hazardous Materials, 2020, 384, 121313.	12.4	39
51	Dynamic flow and pollution of antimony from polyethylene terephthalate (PET) fibers in China. Science of the Total Environment, 2021, 771, 144643.	8.0	39
52	Exposure inequality assessment for PM2.5 and the potential association with environmental health in Beijing. Science of the Total Environment, 2018, 635, 769-778.	8.0	37
53	Combined impacts of freeze–thaw processes on paddy land and dry land in Northeast China. Science of the Total Environment, 2013, 456-457, 24-33.	8.0	36
54	Differences in soil organic carbon dynamics in paddy fields and drylands in northeast China using the CENTURY model. Agriculture, Ecosystems and Environment, 2014, 194, 38-47.	5.3	36

#	Article	IF	CITATIONS
55	In situ remediation of cadmium-polluted soil reusing four by-products individually and in combination. Journal of Soils and Sediments, 2014, 14, 451-461.	3.0	36
56	Long-term agricultural non-point source pollution loading dynamics and correlation with outlet sediment geochemistry. Journal of Hydrology, 2016, 540, 379-385.	5.4	36
57	Toxicity and bioavailability of antimony in edible amaranth (Amaranthus tricolor Linn.) cultivated in two agricultural soil types. Environmental Pollution, 2020, 257, 113642.	7.5	36
58	Combine the soil water assessment tool (SWAT) with sediment geochemistry to evaluate diffuse heavy metal loadings at watershed scale. Journal of Hazardous Materials, 2014, 280, 252-259.	12.4	35
59	Anthropogenic impact on diffuse trace metal accumulation in river sediments from agricultural reclamation areas with geochemical and isotopic approaches. Science of the Total Environment, 2015, 536, 609-615.	8.0	35
60	Effects of soil moisture content on upland nitrogen loss. Journal of Hydrology, 2017, 546, 71-80.	5.4	35
61	Uptake, translocation and phytotoxicity of antimonite in wheat (Triticum aestivum). Science of the Total Environment, 2019, 669, 421-430.	8.0	34
62	Airborne bacterial communities and antibiotic resistance gene dynamics in PM2.5 during rainfall. Environment International, 2020, 134, 105318.	10.0	32
63	Effects of antimony (III/V) on microbial activities and bacterial community structure in soil. Science of the Total Environment, 2021, 789, 148073.	8.0	31
64	Activation of peroxymonosulfate by WTRs-based iron-carbon composites for atrazine removal: Performance evaluation, mechanism insight and byproduct analysis. Chemical Engineering Journal, 2021, 421, 127811.	12.7	30
65	Accumulated effects on landscape pattern by hydroelectric cascade exploitation in the Yellow River basin from 1977 to 2006. Landscape and Urban Planning, 2009, 93, 163-171.	7.5	29
66	Soil respiration and carbon loss relationship with temperature and land use conversion in freeze–thaw agricultural area. Science of the Total Environment, 2015, 533, 215-222.	8.0	29
67	Heavy metal accumulation, geochemical fractions, and loadings in two agricultural watersheds with distinct climate conditions. Journal of Hazardous Materials, 2020, 389, 122125.	12.4	29
68	Endocrine-disrupting chemicals in a typical urbanized bay of Yellow Sea, China: Distribution, risk assessment, and identification of priority pollutants. Environmental Pollution, 2021, 287, 117588.	7.5	29
69	Distribution, source, and ecological risks of polycyclic aromatic hydrocarbons in Lake Qinghai, China. Environmental Pollution, 2020, 266, 115401.	7.5	28
70	Profiling of the spatiotemporal distribution, risks, and prioritization of antibiotics in the waters of Laizhou Bay, northern China. Journal of Hazardous Materials, 2022, 424, 127487.	12.4	28
71	Distribution, partitioning, and health risk assessment of organophosphate esters in a major tributary of middle Yangtze River using Monte Carlo simulation. Water Research, 2022, 219, 118559.	11.3	28
72	Vertical distribution of rare earth elements in a wetland soil core from the Sanjiang Plain in China. Journal of Rare Earths, 2012, 30, 731-738.	4.8	27

#	Article	IF	CITATIONS
73	Integration of multi-sensor data to assess grassland dynamics in a Yellow River sub-watershed. Ecological Indicators, 2012, 18, 163-170.	6.3	27
74	A Statistical Method for Categorical Drought Prediction Based on NLDAS-2. Journal of Applied Meteorology and Climatology, 2016, 55, 1049-1061.	1.5	27
75	Vertical difference of climate change impacts on vegetation at temporal-spatial scales in the upper stream of the Mekong River Basin. Science of the Total Environment, 2020, 701, 134782.	8.0	27
76	Activation of peroxymonosulfate using drinking water treatment residuals modified by hydrothermal treatment for imidacloprid degradation. Chemosphere, 2020, 254, 126820.	8.2	27
77	Higher Fine Particle Fraction in Sediment Increased Phosphorus Flux to Estuary in Restored Yellow River Basin. Environmental Science & Technology, 2021, 55, 6783-6790.	10.0	25
78	Assessment of cadmium pollution and subsequent ecological and health risks in Jiaozhou Bay of the Yellow Sea. Science of the Total Environment, 2021, 774, 145016.	8.0	25
79	Interactions of antimony with biomolecules and its effects on human health. Ecotoxicology and Environmental Safety, 2022, 233, 113317.	6.0	25
80	Long-term cultivation impact on the heavy metal behavior in a reclaimed wetland, Northeast China. Journal of Soils and Sediments, 2014, 14, 567-576.	3.0	24
81	Combined impacts of precipitation and temperature on diffuse phosphorus pollution loading and critical source area identification in a freeze-thaw area. Science of the Total Environment, 2016, 553, 607-616.	8.0	24
82	Changes in fertilizer categories significantly altered the estimates of ammonia volatilizations induced from increased synthetic fertilizer application to Chinese rice fields. Agriculture, Ecosystems and Environment, 2018, 265, 112-122.	5.3	24
83	Regional Non point Source Organic Pollution Modeling and Critical Area Identification for Watershed Best Environmental Management. Water, Air, and Soil Pollution, 2007, 187, 251-261.	2.4	23
84	Drainage optimization of paddy field watershed for diffuse phosphorus pollution control and sustainable agricultural development. Agriculture, Ecosystems and Environment, 2021, 308, 107238.	5.3	23
85	Assessing the Relationship Between Landscape Patterns and Nonpointâ€6ource Pollution in the Danjiangkou Reservoir Basin in China <sup>1</sup> . Journal of the American Water Resources Association, 2012, 48, 1162-1177.	2.4	22
86	Temporal rainfall patterns with water partitioning impacts on maize yield in a freeze–thaw zone. Journal of Hydrology, 2013, 486, 412-419.	5.4	22
87	Impact of crop patterns and cultivation on carbon sequestration and global warming potential in an agricultural freeze zone. Ecological Modelling, 2013, 252, 228-237.	2.5	22
88	Farmland shift due to climate warming and impacts on temporal-spatial distributions of water resources in a middle-high latitude agricultural watershed. Journal of Hydrology, 2017, 547, 156-167.	5.4	22
89	Temporal-spatial variation analysis of agricultural biomass and its policy implication as an alternative energy in northeastern China. Energy Policy, 2017, 109, 337-349.	8.8	22
90	Rainwater characteristics and interaction with atmospheric particle matter transportation analyzed by remote sensing around Beijing. Science of the Total Environment, 2019, 651, 532-540.	8.0	22

#	Article	IF	CITATIONS
91	Vanadium pollution and health risks in marine ecosystems: Anthropogenic sources over natural contributions. Water Research, 2021, 207, 117838.	11.3	22
92	Contents and chemical forms of heavy metals in school and roadside topsoils and road-surface dust of Beijing. Journal of Soils and Sediments, 2014, 14, 1806-1817.	3.0	21
93	Toward a categorical drought prediction system based on U.S. Drought Monitor (USDM) and climate forecast. Journal of Hydrology, 2017, 551, 300-305.	5.4	21
94	Typical herbicide residues, trophic transfer, bioconcentration, and health risk of marine organisms. Environment International, 2021, 152, 106500.	10.0	21
95	A comprehensive assessment of anthropogenic impacts, contamination, and ecological risks of toxic elements in sediments of urban rivers: A case study in Qingdao, East China. Environmental Advances, 2022, 7, 100143.	4.8	21
96	Modified control strategies for critical source area of nitrogen (CSAN) in a typical freeze-thaw watershed. Journal of Hydrology, 2017, 551, 518-531.	5.4	20
97	Occurrence and risk assessment of total mercury and methylmercury in surface seawater and sediments from the Jiaozhou Bay, Yellow Sea. Science of the Total Environment, 2020, 714, 136539.	8.0	20
98	Trophic transfer and dietary exposure risk of mercury in aquatic organisms from urbanized coastal ecosystems. Chemosphere, 2021, 281, 130836.	8.2	20
99	Long-term soil nutrient dynamics comparison under smallholding land and farmland policy in northeast of China. Science of the Total Environment, 2013, 450-451, 129-139.	8.0	19
100	Optimisation of corn straw biochar treatment with catalytic pyrolysis in intensive agricultural area. Ecological Engineering, 2015, 84, 278-286.	3.6	19
101	Organophosphate esters in surface waters of Shandong Peninsula in eastern China: Levels, profile, source, spatial distribution, and partitioning. Environmental Pollution, 2022, 297, 118792.	7.5	19
102	Simultaneous stabilization of Sb and As co-contaminated soil by Fe Mg modified biochar. Science of the Total Environment, 2022, 830, 154831.	8.0	19
103	Spatial and temporal trend of Chinese manure nutrient pollution and assimilation capacity of cropland and grassland. Environmental Science and Pollution Research, 2013, 20, 5036-5046.	5.3	18
104	Geochemical variability of heavy metals in soil after land use conversions in Northeast China and its environmental applications. Environmental Sciences: Processes and Impacts, 2014, 16, 924-931.	3.5	18
105	Watershed water circle dynamics during long term farmland conversion in freeze-thawing area. Journal of Hydrology, 2015, 523, 555-562.	5.4	18
106	Optimization of typical diffuse herbicide pollution control by soil amendment configurations under four levels of rainfall intensities. Journal of Environmental Management, 2016, 175, 1-8.	7.8	18
107	Long-term diffuse phosphorus pollution dynamics under the combined influence of land use and soil property variations. Science of the Total Environment, 2017, 579, 1894-1903.	8.0	18
108	Interactions between rainfall and fine particulate matter investigated by simultaneous chemical composition measurements in downtown Beijing. Atmospheric Environment, 2019, 218, 117000.	4.1	18

#	Article	IF	CITATIONS
109	Watershed diffuse pollution dynamics and response to land development assessment with riverine sediments. Science of the Total Environment, 2019, 659, 283-292.	8.0	18
110	Metabolic process and spatial partition dynamics of Atrazine in an estuary-to-bay system, Jiaozhou bay. Journal of Hazardous Materials, 2021, 414, 125530.	12.4	18
111	Facile co-removal of As(V) and Sb(V) from aqueous solution using Fe-Cu binary oxides: Structural modification and self-driven force field of copper oxides. Science of the Total Environment, 2022, 803, 150084.	8.0	18
112	Vertical and horizontal distribution of soil parameters in intensive agricultural zone and effect on diffuse nitrogen pollution. Soil and Tillage Research, 2014, 144, 32-40.	5.6	17
113	Coupling the Xinanjiang model with geomorphologic instantaneous unit hydrograph for flood forecasting in northeast China. International Soil and Water Conservation Research, 2015, 3, 66-76.	6.5	17
114	Mechanochemical treatment with CaO-activated PDS of HCB contaminated soils. Chemosphere, 2020, 257, 127207.	8.2	17
115	Diffuse nitrogen pollution in a forest-dominated watershed: Source, transport and removal. Journal of Hydrology, 2020, 585, 124833.	5.4	17
116	Influences of Particles and Aquatic Colloids on the Oxidation of Sb(III) in Natural Water. ACS Earth and Space Chemistry, 2020, 4, 661-671.	2.7	17
117	Toxicity and bioavailability of antimony to the earthworm (Eisenia fetida) in different agricultural soils. Environmental Pollution, 2021, 291, 118215.	7.5	17
118	A Supply-Chain Analysis Framework for Assessing Densified Biomass Solid Fuel Utilization Policies in China. Energies, 2015, 8, 7122-7139.	3.1	16
119	Increased ammonia emissions from synthetic fertilizers and land degradation associated with reduction in arable land area in China. Land Degradation and Development, 2018, 29, 3928-3939.	3.9	16
120	Influence of Fe(II) on Sb(III) oxidation and adsorption by MnO2 under acidic conditions. Science of the Total Environment, 2020, 724, 138209.	8.0	16
121	Quantify phosphorus transport distinction of different reaches to estuary under long-term anthropogenic perturbation. Science of the Total Environment, 2021, 780, 146647.	8.0	16
122	Potential of paddy drainage optimization to water and food security in China. Resources, Conservation and Recycling, 2021, 171, 105624.	10.8	16
123	Trophodynamics of arsenic for different species in coastal regions of the Northwest Pacific Ocean: In situ evidence and a meta-analysis. Water Research, 2020, 184, 116186.	11.3	15
124	Optimization of SWAT-Paddy for modeling hydrology and diffuse pollution of large rice paddy fields. Environmental Modelling and Software, 2020, 130, 104736.	4.5	15
125	Considering atmospheric N2O dynamic in SWAT model avoids the overestimation of N2O emissions in river networks. Water Research, 2020, 174, 115624.	11.3	15
126	Insights into the spatiotemporal occurrence and mixture risk assessment of household and personal care products in the waters from rivers to Laizhou Bay, southern Bohai Sea. Science of the Total Environment, 2022, 810, 152290.	8.0	15

#	Article	IF	CITATIONS
127	Farmland–atmosphere feedbacks amplify decreases in diffuse nitrogen pollution in a freeze-thaw agricultural area under climate warming conditions. Science of the Total Environment, 2017, 579, 484-494.	8.0	14
128	Seasonal occurrence, allocation and ecological risk of organophosphate esters in a typical urbanized semi-closed bay. Environmental Pollution, 2021, 290, 118074.	7.5	14
129	Paddy rice ecohydrology pattern and influence on nitrogen dynamics in middle-to-high latitude area. Journal of Hydrology, 2015, 529, 1901-1908.	5.4	13
130	Seasonal variations in atrazine degradation in a typical semienclosed bay of the northwest Pacific ocean. Environmental Pollution, 2021, 283, 117072.	7.5	13
131	Applying Multi-source Remote Sensing Data on Estimating Ecological Water Requirement of Grassland in Ungauged Region. Procedia Environmental Sciences, 2010, 2, 953-963.	1.4	12
132	LUCC and landscape pattern variation of wetlands in warm-rainy Southern China over two decades. Procedia Environmental Sciences, 2010, 2, 1296-1306.	1.4	12
133	Satellite-based estimation of watershed groundwater storage dynamics in a freeze–thaw area under intensive agricultural development. Journal of Hydrology, 2016, 537, 96-105.	5.4	12
134	Typical pesticides diffuse loading and degradation pattern differences under the impacts of climate and land-use variations. Environment International, 2020, 139, 105717.	10.0	12
135	Efficient catalyst prepared from water treatment residuals and industrial glucose using hydrothermal treatment: Preparation, characterization and its catalytic performance for activating peroxymonosulfate to degrade imidacloprid. Chemosphere, 2022, 290, 133326.	8.2	12
136	Accumulated impact assessment of river buffer zone after 30Âyears of dam disturbance in the Yellow River Basin. Stochastic Environmental Research and Risk Assessment, 2013, 27, 1069-1079.	4.0	11
137	SWAT-N2O coupler: An integration tool for soil N2O emission modeling. Environmental Modelling and Software, 2019, 115, 86-97.	4.5	11
138	Differences in soil water content and movement drivers of runoff under climate variations in a high-altitude catchment. Journal of Hydrology, 2020, 587, 125024.	5.4	11
139	Arsenic profile distribution of the wetland argialbolls in the Sanjiang plain of northeastern China. Scientific Reports, 2015, 5, 10766.	3.3	10
140	A comparison of general circulation models and their application to temperature change assessments in a high-latitude agricultural area in northeastern China. Climate Dynamics, 2016, 47, 651-666.	3.8	10
141	Simultaneous electrochemical determination of Sb(III) and Sb(V) in Water samples: Deposition potential differences and Sb(III) photooxidation characteristics. Sensors and Actuators B: Chemical, 2020, 305, 127454.	7.8	10
142	Role of freeze-thaw cycles and chlorpyrifos insecticide use on diffuse Cd loss and sediment accumulation. Scientific Reports, 2016, 6, 27302.	3.3	9
143	Soil respiration characteristics in different land uses and response of soil organic carbon to biochar addition in high-latitude agricultural area. Environmental Science and Pollution Research, 2016, 23, 2279-2287.	5.3	9
144	Integrating hydrological, landscape ecological, and economic assessment during hydropower exploitation in the upper Yangtze River. Science of the Total Environment, 2021, 767, 145496.	8.0	9

#	Article	IF	CITATIONS
145	Phosphorus Fractions and Availability in an Albic Bleached Meadow Soil. Agronomy Journal, 2013, 105, 1451-1457.	1.8	8
146	Multivariate interactions of natural and anthropogenic factors on Cd behavior in arable soil. RSC Advances, 2015, 5, 41238-41247.	3.6	8
147	Anthropogenic and lithogenic fluxes of atmospheric lead deposition over the past 3600 years from a peat bog, Changbai Mountains, China. Chemosphere, 2019, 227, 225-236.	8.2	8
148	Mechanism of birnessite-promoted oxidative dissolution of antimony trioxide. Environmental Chemistry, 2020, 17, 345.	1.5	8
149	Synergetic loss of heavy metal and phosphorus: Evidence from geochemical fraction and estuary sedimentation. Journal of Hazardous Materials, 2021, 416, 125710.	12.4	7
150	Sorption dynamics, geochemical fraction and driving factors in phosphorus transport at large basin scale. Journal of Cleaner Production, 2021, 294, 126111.	9.3	6
151	Baseline, enrichment, and ecological risk of arsenic and antimony in the Jiaozhou Bay, a semi-enclosed bay of the Yellow Sea, China. Marine Pollution Bulletin, 2021, 168, 112431.	5.0	6
152	Microbial community structure and metabolic potential in the coastal sediments around the Yellow River Estuary. Science of the Total Environment, 2022, 816, 151582.	8.0	6
153	Horizontal planetary mechanochemical method for rapid and efficient remediation of high-concentration lindane-contaminated soils in an alkaline environment. Journal of Hazardous Materials, 2022, 436, 129078.	12.4	6
154	Enhanced release, export, and transport of diffuse nutrients from litter in forested watersheds with climate warming. Science of the Total Environment, 2022, 837, 155897.	8.0	6
155	Predictive ability of climate change with the automated statistical downscaling method in a freeze–thaw agricultural area. Climate Dynamics, 2019, 52, 7013-7028.	3.8	5
156	Rainfall stimulates large carbon dioxide emission during growing season in a forest wetland catchment. Journal of Hydrology, 2021, 602, 126892.	5.4	5
157	Quantitative source identification and environmental assessment of trace elements in the water and sediment of rivers flowing into Laizhou Bay, Bohai Sea. Marine Pollution Bulletin, 2022, 174, 113313.	5.0	5
158	Diffuse nutrient export dynamics from accumulated litterfall in forested watersheds with remote sensing data coupled model. Water Research, 2022, 209, 117948.	11.3	5
159	Historical records of trace metals in two sediment cores of Jiaozhou Bay, north China. Marine Pollution Bulletin, 2022, 175, 113400.	5.0	5
160	Deep insight into the Sb(III) and Sb(V) removal mechanism by Fe–Cu-chitosan material. Environmental Pollution, 2022, 303, 119160.	7.5	5
161	Vertical Distribution of Lead and Mercury in the Wetland Argialbolls of the Sanjiang Plain in Northeastern China. PLoS ONE, 2015, 10, e0124294.	2.5	4
162	Spatiotemporal variations in phosphorus concentrations in the water and sediment of Jiaozhou Bay and sediment phosphorus release potential. Science of the Total Environment, 2022, 806, 150540.	8.0	4

#	Article	IF	CITATIONS
163	Desert disturbance assessments of regional oil exploitation by Aster and ETM+ images in Taklimakan Desert China. Environmental Monitoring and Assessment, 2008, 144, 159-168.	2.7	3
164	Dryland Soil Hydrological Processes and Their Impacts on the Nitrogen Balance in a Soil-Maize System of a Freeze-Thawing Agricultural Area. PLoS ONE, 2014, 9, e101282.	2.5	3
165	Ammonia volatilization modeling optimization for rice watersheds under climatic differences. Science of the Total Environment, 2021, 767, 144710.	8.0	3
166	Spatial impacts of climate factors on regional agricultural and forestry biomass resources in north-eastern province of China. Frontiers of Environmental Science and Engineering, 2016, 10, 1.	6.0	2
167	Impact of Regional Management Alternatives and Land Conversion on the Net Primary Productivity in Heilongjiang Province, China. Journal of Environmental Accounting and Management, 2016, 4, 45-58.	0.5	2
168	Forest leaf litter nutrient discharge patterns in snowmelt surface runoff and watershed scale remote sensed simulation. Science of the Total Environment, 2022, 839, 156356.	8.0	2
169	Chinese Strategic Environmental Assessment system and its application in water resources development plan of the Yellow River. International Journal of Environment and Waste Management, 2010, 5, 181.	0.3	1
170	Typical agricultural diffuse herbicide sorption with agricultural waste-derived biochars amended soil of high organic matter content. , 2016, 92, 156-156.		1
171	Satellite Remote Sensing Drought Monitoring and Predictions over the Globe. , 2016, , 259-296.		1
172	Experimental Studying Polluted Water Treatment in Northern China. Water Resources, 2005, 32, 456-459.	0.9	0
173	Characteristics analysis of first flush effect on runoff pollutants from different urban underlying surfaces. , 2010, , .		0
174	Integrated Ecohydrological Models in Aquatic Ecosystems. Water (Switzerland), 2022, 14, 204.	2.7	0